Supporting Information

Lin et al. 10.1073/pnas.0910243107

SI Text

Characterization of Surface Modification by Fluorescence Imaging. The micropatterns on a Si substrate were fabricated by spin-coating two-layer photoresists, LOR5B and S1813, on the Si wafer and by photolithographic writing to create a set of square patterns ($40 \times 40\ \mu m^2$) (Fig. S1*A*). Before surface modification, the layer of S1813 on the patterned substrate was removed by washing with acetone. The Si substrate was then cleaned with oxygen plasma (30 W and 50 sccm O_2 for 60 s). For surface modification, the patterned squares were modified with APTMS, and the surrounding photoresists were lifted off with a PG remover (Fig. S1*B*). Subsequently, the APTMS-immobilized Si substrate was subjected to GSH modification with the same procedures as described in the Materials and Methods section of the main text.

A microscopic fluorescence imaging technique was used to prove successful surface modification. The GSH-modified substrate was first immersed in 1X PS supplemented with 500 nM GST (Sigma) for 1 hr and then washed with 1X PS supplemented with 1% bovine serum albumin (BSA, Sigma) to prevent non-specific binding. Subsequently, the substrate was stained with FITC-labeled goat polyclonal IgG against GST (Abcam) in 1X PS for 1 hr. After washing with 1X PS and blow-drying with N_2, a fluorescent image of the stained substrate was acquired (as shown in Fig. 2*A* of the main text) using a phase-contrast, upright fluorescence microscope (Zeiss, Axioplan 2 Imaging MOT) equipped with an intensified Cool Snap EZ charged coupled device camera.

Detection of GST and CaM-GST using SiNW-FETs without modified GSH. Due to its low ionic strength, 0.1X PS was weakly resistant to the pH change upon addition of a large amount of solutes. As a result, the pH level of 0.1X PS was changed from 7.4 to 4.5 when 1 mM GSH was dissolved in the 0.1X PS. As shown in Fig. S2*A* and *B*, a bare SiNW-FET was initially immersed in GSH (1 mM in 0.1X PS, pH 4.5) and increased its conductance after the introduction of 0.1X PS at pH 7.4, which was attributed to the pH variation (1). To clarify the effect of high GSH dose on the bare SiNW-FET, the pH level of the 1 mM GSH in 0.1X PS was adjusted to 7.4. As shown in Fig. S2*C*, no measurable ΔG was detected by the bare SiNW-FET when the GSH solution (1 mM in 0.1X PS, pH 7.4) was replaced by 0.1X PS at pH 7.4, suggesting that the ionic strength of 1 mM GSH made an inconsiderable contribution to the ΔG of the SiNW-FET. Comparatively, it was not until the addition of 10 times more concentrated GSH solution (10 mM in 0.1X PS, pH 7.4) that the bare SiNW-FET had a approximately 4% variation in ΔG as shown in Fig. S2*D*.

It was also noted that a bare SiNW-FET showed no response to either GST (5 μM in 0.1X PS, pH 7.4; Fig. S2*A*, *C*, and *D*) or GST-CaM (400 nM in 0.1X PS, pH 7.4; Fig. S2*B*). These results demonstrated that GST and CaM-GST were specifically recognized only by the GSH/SiNW-FET, as shown in Fig. 2*B* and *C* of the main text, respectively.

Interference of the Metal Ions Present in the Phosphate Buffer with the Calmodulin Experiments. As shown in Fig. S3, the conductance decreased in the p-type GSH/SiNW-FET after the addition of 200 nM CaM-GST dissolved in 0.1X PS, which is contrary to the increase in conductance observed when 400 nM CaM-GST was dissolved in 0.1X PS supplemented with 0.5 mM EDTA (Fig. 2*C* of the main text). It was suspected that trace amounts of Ca^{2+} or other metal ions present in the deionized water and/or in the chemicals used in the experiments might be responsible for the contradictory changes in conductance. Therefore, care was taken to avoid this kind of interference in the calmodulin sensing experiments.

Detection of Ca^{2+} using the GST/SiNW-FET. After completing the electrical measurements of the various metal ions with the CaM/SiNW-FET, the device was washed with 1 mM GSH solution in order to remove the used CaM-GST. The GSH/SiNW-FET device was then immersed in a 500 nM GST solution for 30 min to form the GST/SiNW-FET, which had no electrical response to Ca^{2+}, as shown in Fig. S4.

Association of an N-type Ca^{2+} Channel with CaM as Demonstrated by Fluorescence Imaging. The micropatterns on a Si substrate were first modified with GSH and then associated with CaM-GST, according to the procedures described in the Materials and Methods section of the main text. After diluting the cell extract containing 34 μg/μL N-type Ca^{2+} channels 20 times in 1X PBS supplemented with 10^{-4} M Ca^{2+}, the extract was incubated with the CaM-immobilized substrate for 1 hr. PBS (1X) supplemented with 10^{-4} M Ca^{2+} was used in this labeling experiment. To minimize non-specific binding, the substrate was washed with the same buffer containing 1% BSA (Sigma) for 30 min and then stained with a Ca^{2+} channel-specific rabbit polyclonal IgG (Santa Cruz Biotechnology, diluted 100X in PBS) antibody for 2 hr. Finally, the substrate was stained with FITC-conjugated mouse anti-rabbit IgG for 1 hr. The stained substrate was then washed and blow-dried with N_2. The labeled substrate was analyzed under a fluorescence microscope for imaging (Fig. S5).

Fabrication and Electrical Characterization of the SiNW-FET. Boron-doped SiNWs (Si:B $=4000:1$) were synthesized catalytically (assisted by 20 nm gold nanoparticles) in a chemical vapor deposition reaction at 460 °C via a vapor-liquid-solid growth mechanism from silane (SiH_4) and diborane (B_2H_6) precursors (2–4). The crystallinity of the as-synthesized SiNWs of 30–60 nm in diameter was characterized by high-resolution transmission electron microscopy (Philips/FEI Tecnai 20 G2 at 200 KV). Before the fabrication of the SiNW-FET devices, the as-synthesized SiNWs were ultrasonicated in ethanol and then dispersed on a highly boron-doped Si wafer ($1.7 \times 1.7\ cm^2$) with a 400 nm SiO_2 layer. The SiNW-FET devices were fabricated following standard photolithographic procedures (2). The metal leads were made by the deposition of Ni (70 nm thick) and Al (100 nm thick). The surface of the Al layer was later oxidized to form an Al_2O_3 film several nanometers thick, serving as an insulating coat for the prevention of electric leakage during sensing experiments. The as-fabricated SiNW-FET chip was then annealed in a rapid thermal annealer (Ulvac, Mila-3000) with 10% H_2 and 90 % N_2 forming gases at 360 °C for 1 min, in order to form an Ohmic contact between the Ni leads and the SiNWs. The electrical characteristics of the as-fabricated SiNW-FET devices are presented in Fig. S6.

1. Cui Y, Wei QQ, Park HK, Lieber CM (2001) Nanowire nanosensors for highly sensitive and selective detection of biological and chemical species. *Science* 293:1289–1292.

2. Patolsky F, Zheng GF, Lieber CM (2006) Fabrication of silicon nanowire devices for ultrasensitive, label-free, real-time detection of biological and chemical species. *Nat Protoc* 1:1711–1724.

3. Patolsky F, Timko BP, Zheng GF, Lieber CM (2007) Nanowire-based nanoelectronic devices in the life sciences. *MRS Bull* 32:142–149.

4. Yang YH, Wu SJ, Chiu HS, Lin PI, Chen YT (2004) Catalytic growth of silicon nanowires assisted by laser ablation. *J Phys Chem B* 108:846–852.

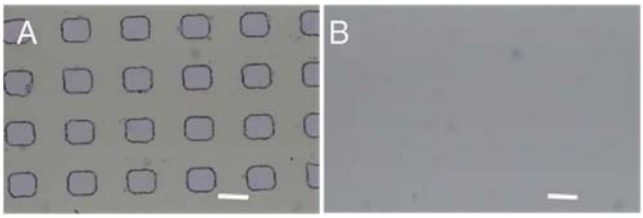

Fig. S1. Fabrication of micropatterns on the Si substrate for fluorescence imaging experiments. Optical images are shown for (*A*) the micropatterns fabricated using a standard photolithographic procedure and (*B*) the APTMS-immobilized micropatterns after removal of the surrounding photoresists. Scale bars represent 50 μm.

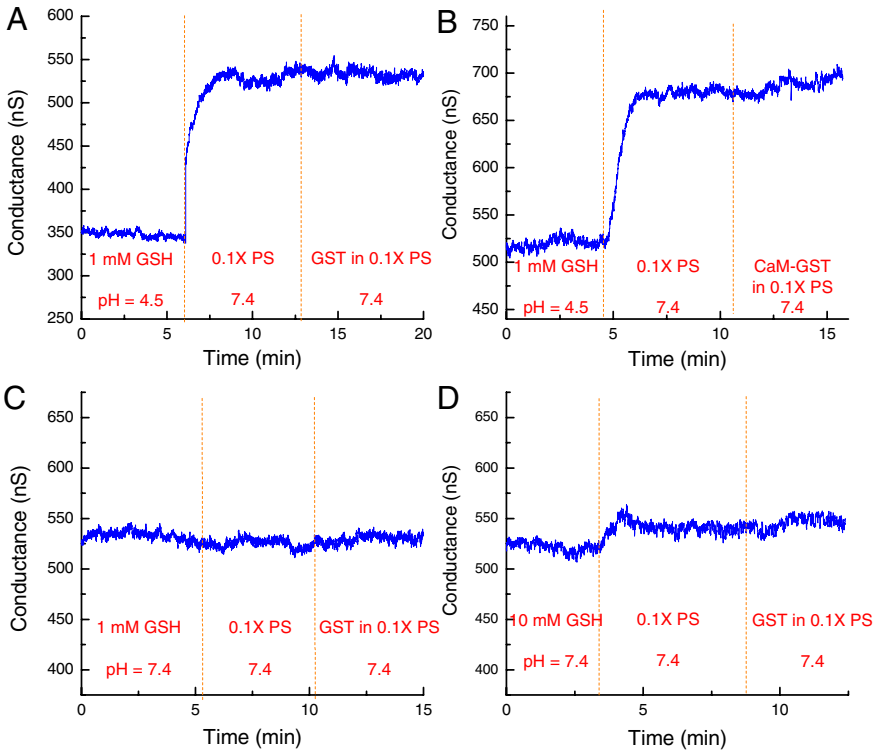

Fig. S2. Detection of GST and CaM-GST by a bare SiNW-FET. The real-time detection of (*A*) GST (5 μM in 0.1X PS, pH 7.4) and (*B*) GST-CaM (400 nM in 0.1X PS, pH 7.4) with a bare SiNW-FET are shown. The bare SiNW-FET showed no response to GST or CaM-GST. The prominent increase in the ΔG of the bare SiNW-FET was mainly attributed to the deprotonation of the silanol groups on the SiNW surface due to the pH variation from 4.5 to 7.4. In contrast, the change of ionic strength from varying the concentration of GSH from (*C*) 1 mM to (*D*) 10 mM, in 0.1X PS at pH 7.4, made little difference to the ΔG of the FET sensor.

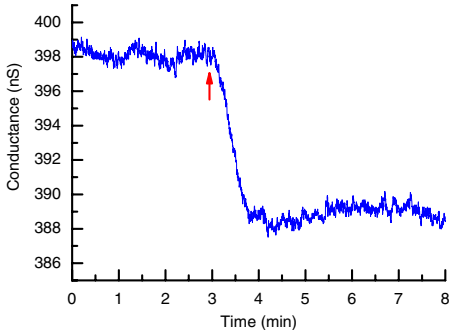

Fig. S3. Effects of residual metal ions in the buffer solution in the calmodulin experiments. Real-time electrical measurements of the binding of 200 nM CaM-GST to a GSH/SiNW-FET in 0.1X PS with $\lambda_D = 6.1$ nm. The red arrow indicates the arrival of the CaM-GST solution.

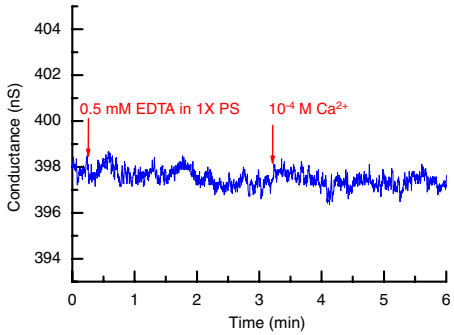

Fig. S4. Detection of Ca^{2+} by the GST/SiNW-FET. Real-time electrical measurements were conducted using a GST/SiNW-FET for the detection of Ca^{2+} in 1X PS supplemented with 0.5 mM EDTA.

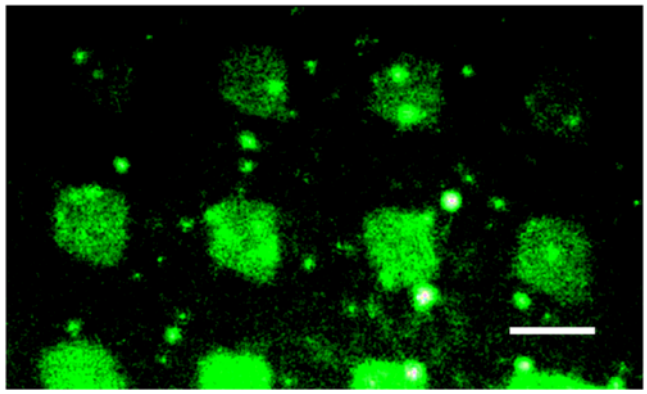

Fig. S5. Binding of N-type Ca^{2+} channels to CaM-modified micropatterns. The green fluorescence on the micropatterns indicates the association of the FITC-tagged Ca^{2+} channel with the CaM-modified micropatterns. The scale bar represents 50 μm.

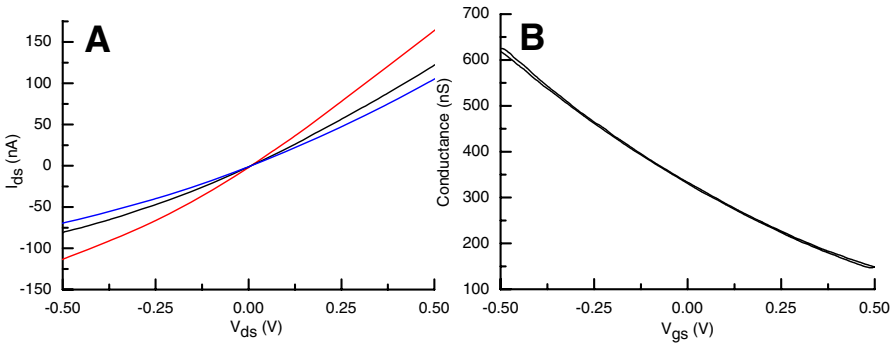

Fig. S6. Electric transport properties of the as-fabricated SiNW-FET. (*A*) A source-drain current (I_{ds}) vs. source-drain voltage (V_{ds}) plot at different gate voltages (V_{gs}) for a typical SiNW-FET device. The red, black, and blue curves represent the electrical measurements at $V_{gs} = -10$, 0, and 10 V, respectively. The linear dependence of the I_{ds} on the varied V_{ds} indicates an Ohmic contact between the Ni leads and the SiNW. (*B*) Conductance vs. V_{gs} was recorded in water for the same SiNW-FET device at $V_{ds} = 30$ mV, where a transconductance of 480 nS was calculated for this p-type FET device.